Seismic performance of non-ductile reinforced concrete frame detailing – a Taiwanese example

B.A. Hidayat
Department of Civil Engineering, National Cheng Kung University, Tainan, Taiwan.
Department of Civil Engineering, Universitas Diponegoro, Semarang, Indonesia.

F.-P. Hsiao, P.-W. Weng & W.-C. Shen
National Center for Research on Earthquake Engineering, Taipei, Taiwan.

H.-T. Hu, P. Pita & L. Nugroho
Department of Civil Engineering, National Cheng Kung University, Tainan, Taiwan.

A.L. Han
Department of Civil Engineering, Universitas Diponegoro, Semarang, Indonesia.

Y. Haryanto
Department of Civil Engineering, Universitas Jenderal Soedirman, Purwokerto, Indonesia.
National Center for Research on Earthquake Engineering, Taipei, Taiwan.
Department of Civil Engineering, National Cheng Kung University, Tainan, Taiwan.

ABSTRACT

Reinforced concrete (RC) frames constructed before ductility requirements were established are prone to structural collapse during earthquakes. Significant damage often occurs in the beam-column joints (BCJs), accompanied by critical deterioration of columns. This study investigates the seismic performance and failure mechanisms of non-ductile RC exterior BCJs and adjacent columns, referencing a real structure in Taiwan that collapsed in the 2016 Mei-Nong earthquake. Results indicate inadequate seismic response, evidenced by extensive cracking and crack propagation in the upper and lower sections of the columns under lateral loads. The BCJ specimens exhibited a progressive loss of stiffness and strength, eventually failing in shear at the joint. Deformability and energy dissipation also proved insufficient under seismic load. These findings

highlight the vulnerabilities of non-ductile RC frames during seismic events and underscore the need for enhanced detailing to improve resilience.

1 INTRODUCTION

Due to its location on the Pacific ring of fire, Taiwan experiences significant seismic activity, with catastrophic impacts in the past. Furthermore, numerous structures collapsed during the Chi-Chi earthquake in 1999, the 2016 Meinong earthquake, and various other significant seismic events. Among these, the majority of the collapsed structures were built using reinforced concrete (RC) frames (Xue 2000, Zepeda and Hagen, 2016). The damage frequently occurred in the beam-column joints (BCJs), often accompanied by significant column damage, due to inadequate ductile detailing in existing concrete frame structures. This defect frequently manifested in the lower levels of structures featuring larger openings and increased story heights. This condition results in reduced structural stiffness and strength, leading to a soft-story mechanism.

Numerous researches have investigated the seismic performance of RC columns characterized by poor detailing practices, which leads to non-ductile behaviour. Different amounts and detailing layouts of transverse reinforcements used in column specimens have been investigated (Liao et al., 2017, Rajput and Sharma, 2017). Larger spacing of tie bars allows dilation of the concrete core and exhibits poor performance against cyclic loading. In addition, a close transverse reinforcement detailing layout is a crucial factor to ensure ductile behaviour in RC columns. The added confinement provided by transverse bars enhances the crack prevention, energy dissipation capacity, and strength of column specimens.

The cyclic behaviour of RC BCJs holds significant importance in the performance of this structures, and has led to various experimental studies focused on poorly detailed exterior beam-column joints. One of the initial evaluations on external RC BCJs subjected to seismic loading was carried out in New Zealand (Park and Paulay,1973), and focused on the impact of the transverse reinforcement on the seismic performance of these elements. Since then, additional investigations were conducted on BCJs, examining a range of parameters such as, the beam longitudinal reinforcement ratio, joint geometries, joint shear demands, and anchorage details (Shafaei et al., 2014, Li et al., 2015, Faleschini et al., 2017). The findings of these studies indicated that joints exhibiting inadequate seismic reinforcement detailing predominantly experienced failure due to bond-slip and joint shear mechanisms. The reduced energy dissipation capacity for specimens lacking seismic detailing was also documented. The correct anchorage length for the longitudinal beam rebars and their hooked ends, along with the inclusion of transversal reinforcement in the joint core, are essential for ensuring effective anchorage and improving the performance of a BCJ component under seismic loads.

Although numerous studies have examined the seismic performance of non-ductile detailing RC frames, a comprehensive understanding of the behaviour of these frames remains essential. This paper aims to expand upon the findings of several earlier studies (Shen et al., 2018, Hidayat et al., 2020, Hidayat et al. 2021, Hidayat et al. 2022) into the structural investigation of the specified RC members. These earlier publications included the shaking table tests for a half-scale three-story building resembling the Weiguan Jinlong tower in Tainan City, Taiwan, that collapsed during the 2016 Meinong Earthquake. The building's original structural design lacked ductility, making it seismically vulnerable. Under current study, several non-ductile and inadequately designed RC columns and BCJs with the Weiguan Jinlong Tower detailing were tested under the quasi-static testing method, conducted by the Multi-Axial Testing System (MATS) at the National Center for Research on Earthquake Engineering Laboratory in Tainan City. The prototypes were extracted from the external columns on the first floor and the exterior BCJ components of the three-story building that underwent testing on the shaking table in the earlier publications.

2 EXPERIMENTAL PROGRAM

2.1 Specimen configuration

The column specimens, resembling the original building detailing, were designed with a length of 260 cm, featuring varying cross-sectional areas: 30×30 cm for the smaller column labelled as C-A, and 30×75 cm for the larger column identified as C-B. The BCJ specimens consisted of C-A and C-B columns, each measuring 410 cm in length, connected to a beam with dimensions of 25×40 cm and a length of 150 cm, referred to as BCJ-A and BCJ-B, respectively. Table 1 presents the specifics of longitudinal and transverse reinforcement of the RC specimens. The concrete exhibited a compressive strength of 21.96 MPa at 28 days. The ultimate strength, yield strength, and elastic modulus of the steel reinforcements were determined to be 504.7 MPa, 454.3 MPa, and 227.15 GPa for the 19-mm-diameter bar, and 388.5 MPa, 349.7 MPa, and 174.85 GPa for the 10-mm-diameter bar, respectively. These values may be regarded as a low-grade reinforcement. Stirrups and cross-ties spaced 120 and 240 mm, respectively, acted as a representation of the pre-ductile reinforcement detailing on columns. Additionally, it was also noted that the 20-mm concrete cover was less than the ACI 318-19 (2019) recommendations. However, as seen in Table 1, both columns and beams were built with geometric reinforcement ratios of 2.53 and 2.85%, respectively, which met the ACI 318-19 (2019) minimum recommendations. Lack of shear reinforcement and inadequate anchorage within the joint core, as well as the presence of a strong beam with a weak column, were indicative of poor seismic design practices.

Table 1: Details of column and beam–column joints specimens

Specimen	Longitudinal rebars	Stirrup rebars	Crossties rebars	Cross-section (cm)	BCJ reinforcement detailing (cm) (Pita, 2018)
C-A 300x300	8 D19	D10 - 120	D10 - 240	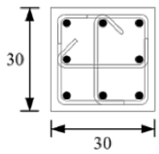	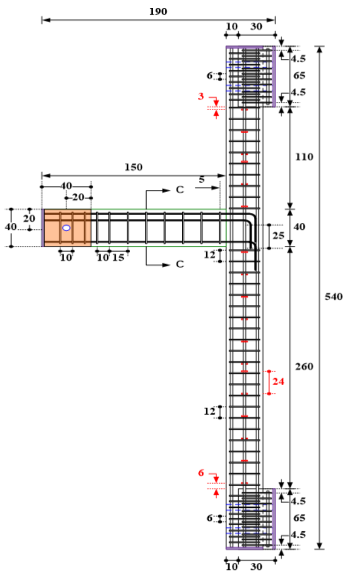
C-B 300x750	20 D19	D10 - 120	D10 - 240	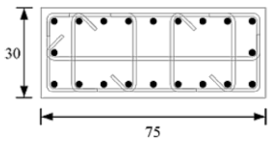	
Beam 250x400	Top: 6 D19 Bottom: 4 D19	D10 - 150	-	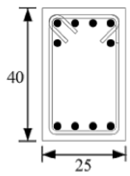	

2.2 Experimental test setup

2.2.1 Columns

To examine the cyclic behaviour of the columns individually, C-A and C-B were tested vertically inside the MATS, as shown in Figure 1. A range of sophisticated optical measurement sensor systems track the column's deformations during the test, including two strain part devices installed at both column ends to measure the displacement of the column and thirty motion tracker devices to measure the deformation of the column close to the bases. A constant axial load of 237 kN was applied in each specimen to represent the weight and additional mass at the first-floor of the three-story building specimen. Using the displacement-controlled mode hydraulic actuators, MATS was utilized to conduct a quasi-static test once the load application was accomplished. The loading procedure is based on the ACI 374.1-05 standard code (2019). At every loading stage, three completely reversed cycles were added.

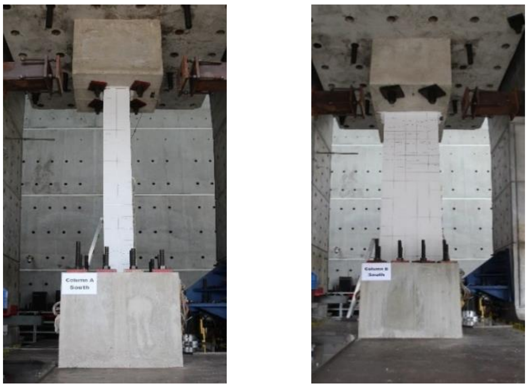

Figure 1: Specimen configuration for C-A 300x300 mm and C-B 300x750 mm utilizing MATS

2.2.2 Beam–column joints

This study investigates the effect of transversal reinforcement on the seismic performance of BCJs, specifically where the joint core lacks transversal rebars. The specimens were evaluated in the MATS with the beam positioned vertically and the column horizontally, as shown in Figure 2. The pinned hinge at the beam end was built as a swivel connector placed 1.3 m from the column face and connected to a load cell to simulate beam and column support conditions. Both joints were constructed with pinned hinge mechanisms to account for the rotation effect, and the supporting structure was built to let the column to exhibit vertical deformation. The bottom portion of the specimen bears the machine's lateral load. The specimens were equipped with motion tracker devices to record joint distortion, strain gauge devices to measure strain, strain part devices to assess beam deflection, and the Linear Variable Displacement Transducer (LVDT) to observe column slide and beam rotation. According to ACI 374.2R-13 (2013), the lateral loading methodology used displacement-controlled stages at 0.25, 0.375, 0.5, 0.75, 1, 1.5, 2, 3, 4, 5, 6, and 7%.

Figure 2: BCJ specimen test configuration utilizing MATS

3 EXPERIMENTAL RESULTS

3.1 Failure mechanisms

The C-A and C-B specimens developed minor flexural cracks at the lower end, indicating crack propagation. This process occurred gradually at drift ratios of 0.5% and 0.25%, respectively, and subsequently progressed to diagonal cracks at drift ratios of 1% and 0.5%, respectively. As drift ratio increased, crack width increased. The maximum lateral loads for the two specimens were recorded at 96.86 kN for C-A and 225.24 kN for C-B, both occurring at a 3% drift ratio. The experiment was carried on at drift ratios of 8% for C-A and 4% for C-B. It was determined that C-B was unable to manage cracks because of rapid propagation and increases in crack width, which caused the test to end more soon than it would have otherwise. Upon conclusion the test of the C-A specimen, the most significant crack was observed at the junction of the column and the bottom base, suggesting that there was a slip of the longitudinal bars. Furthermore, in the case of the C-B specimens, the most significant crack was observed near the top, manifesting as splitting cracks. The C-A specimen exhibited failure in flexural mode, while the C-B specimen was characterized by shear failure. The C-A specimen exhibited a ductile response in contrast to the C-B specimen.

In both BCJ specimens, the initial cracks appeared in the joint area of the BCJ-A specimen, while in the BCJ-B specimen, they formed on the column face 700 mm away from the joint zone, at a drift ratio of 0.25%. This manifested as flexural cracks measuring 0.25 mm in width. Diagonal cracks in both specimens then emerged as a result of concrete crushing, deterioration of the bond in the beam's bottom reinforcement, and degradation of the lateral ultimate load. The fissures emerging around the joint area of the column resulted in the anchorage length of the beam adjacent to the column face being insufficient. The broader diagonal fractures observed at the base of the joint region suggest a decline in the joint's stiffness and its ability to resist moments. The BCJ-A achieved a peak load of 100.40 kN, which aligned with a drift ratio of 2% in the positive direction, persisting until the test concluded at a 5% drift ratio. Furthermore, the peak lateral load recorded for the BCJ-B was 157.57 kN, corresponding to a drift ratio of 3% in the positive direction, with the test concluding at a drift ratio of 7%. The main failure mechanism observed in both specimens was attributed to diagonal shear cracking within the joint zone, resulting from an inadequate quantity of joint shear transverse reinforcement. These results are identical to the study conducted by (Tonidis et al., 2024). Figure 3 illustrates the final crack development for all specimens.

(a) C-A at 8% drift ratio (b) C-B at 4% drift ratio (c) BCJ-A at 5% drift ratio (d) BCJ-B at 7% drift ratio

Figure 3: The final crack pattern at of the column and BCJ specimens, corresponding to different drift ratio

3.2 Hysteretic response

The hysteretic curves of column specimens illustrated in Figure 4 exhibit distinct behavioural responses. Specimen C-B demonstrated a faster degradation, reduced drift capacity and enhanced peak strength relative to specimen C-A. The issue arises from the experimental test to end more quickly for the C-B specimen, which can no longer endure the rapid crack propagation, as depicted in Figure 3. Furthermore, the C-A specimen demonstrated a higher hysteretic loop area characterized by flexural failure, as evidenced by a gradual 12% reduction in strength upon reaching the maximum load. The C-B specimen exhibited a 48% reduction in strength once it exceeded the maximum load, resulting from a substantial decrease in stiffness and strength as displacement increased, with a failure mode primarily linked to shear failure. However, the hysteretic curves of the BCJ-A and BCJ-B specimens exhibited comparable responses, as illustrated in Figure 4. Nonetheless, both specimens demonstrated a slight decline in stiffness and strength, as evidenced by the reduction in load upon reaching the maximum load capacity. The degradation progressed steadily with the increase in input displacement until the specimen ultimately failed in shear at the joint region.

According to ACI 374.2R-13 (2013), reinforced concrete frames are permitted to exhibit a drift ratio of as much as 4%. This value represents the threshold of structural performance regarding a specific level of collapse prevention that reinforced concrete structures undergo during seismic loading, and it can be viewed as a point of ultimate failure. Analysis of Figure 4 reveals that the C-B specimen exhibited a lesser degree of compliance with the established provisions, as it experienced failure before reaching the 4% drift ratio. In contrast, the C-A specimen and both BCJ specimens adhered to the provisions effectively.

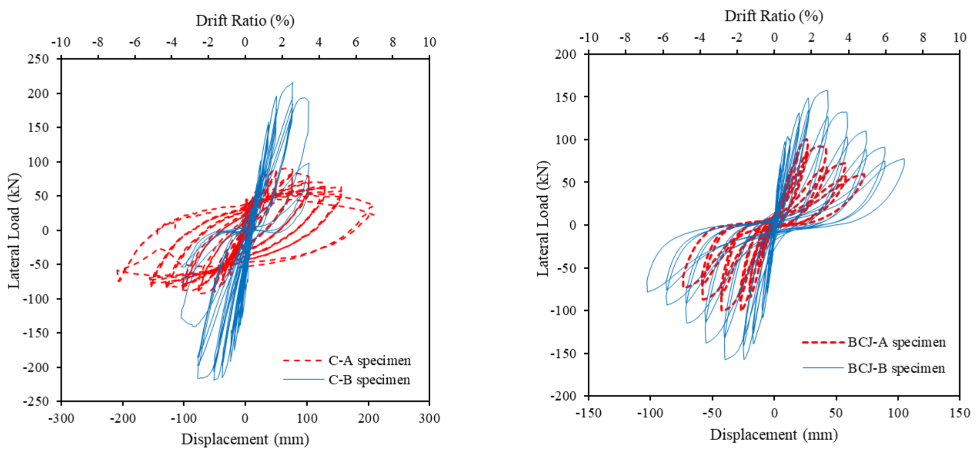

(a) Column specimens C-A and C-B *(b) BCJ specimens BCJ-A and BCJ-B*

Figure 4: Hysteretic response of lateral load versus displacement with corresponding drift ratio

3.3 Beam Rotation

To monitor the beam's rotation in the plastic hinge region, two LVDTs were installed on either side of the beam positioned on top of the column near the joint location. The beam rotation, symbolized as rad, was subsequently calculated using Equation (1), whereby ΔL_1 and ΔL_2 represent the shortening and elongation recorded by the LVDTs, and L_0 denotes the length of the beam to the hinge location. The applied moment is derived by multiplying the lateral load by the beam length measured to the hinge point. Furthermore, Figure 5 was constructed by integrating the beam rotation and moment along the X and Y-axis in a specific curve.

$$rad = \frac{average(\Delta L_1 + \Delta L_2)}{L_0} \tag{1}$$

The findings from Figure 5 demonstrated significant beam rotation for the BCJ-A specimen, attributed to the weak column and strong beam mechanism. This leads to reduced stiffness in BCJ-A relative to BCJ-B. Moreover, both specimens exhibit a comparable rotation of 0.0002 rad under differing applied moments of 70 kNm for BCJ-A and 90 kNm for BCJ-B.

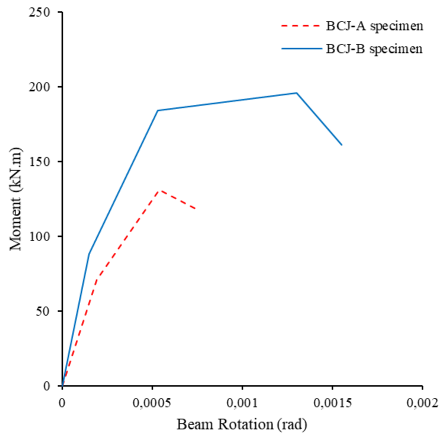

Figure 5: The relationship between beam moment and beam rotation for the BCJ-A and BCJ-B specimens

3.4 Dissipated energy

The energy dissipation measured for each specimen corresponds to a displacement of approximately 70 mm achieved during the testing process. The value was obtained from the displacement point at which the maximum lateral load was reached in the hysteresis loop, as indicated in Figure 4. The C-B specimen exhibited a 47% difference in dissipated energy compared to the C-A specimen, measuring 67 kNm against 128 kNm. This difference can be attributed to the difference in section capacities. Among the BCJ specimens, the BCJ-B specimen exhibited a 30% difference in dissipated energy relative to the BCJ-A specimen, with values recorded at 22 kNm and 33 kNm, respectively. This further confirmed the concept that a strong column paired with a weak beam mechanism, as seen in the BCJ-B specimen, is more efficient due to its enhanced capacity to withstand lateral displacement during seismic loading. The increase of dissipated energy is characterised by the postponement of crack propagation and the yield and ultimate load capacity.

4 CONCLUSIONS

This study uses quasi-static testing to understand the seismic behaviour of poorly detailed RC frame subassemblies and individual columns resembling a recently collapsed building during the 2018 Meinong Earthquake. The larger stirrup spacing in the columns and lack of joint transverse reinforcement indicate poor detailing practices. The columns C-A and C-B specimens, tested in double bending exhibited failure in the flexural mode and shear failure, respectively. The inadequate confinement at column ends promoted the expansion of the concrete core at increasing drift ratios, which in turn led to reduced flexural strength and reduced displacement capacities. The cracking mechanisms and energy dissipation characteristics were recorded for each specimen. The premature failure of BCJ specimens inhibited the columns from hinging, leading to lower deformation capacity, which may have resulted in a different and more favourable outcomes. The joint shear failure observed in the BCJ specimens primarily resulted from an absence of joint transverse rebar within the joint zone, which hindered the development of shear transfer mechanisms.

REFERENCES

ACI 318-19 (2019). "*Building Code Requirements for Structural Concrete and Commentary*". American Concrete Institute. Farmington Hills, Michigan, USA.

ACI 374.1-05 (2019). "*Acceptance Criteria for Moment Frames Based on Structural Testing and Commentary (Reapproved 2019)*". American Concrete Institute. Farmington Hills, Michigan, USA.

ACI 374.2R-13 (2013). "*Guide for Testing Reinforced Concrete Structural Elements under Slowly Applied Simulated Seismic Loads*". American Concrete Institute. Farmington Hills, Michigan, USA.

Faleschini F, Bragolusi P, Zanini MA, Zampieri P and Pellegrino C (2017). "Experimental and numerical investigation on the cyclic behavior of RC beam column joints with EAF slag concrete". *Engineering Structures*, **152**: 332-347.

Hidayat BA, Hu H-T, Hsiao F-P, Han AL, Pita P, Haryanto Y (2020). "Seismic performance of non-ductile detailing RC frames: An experimental investigation". *Earthquake and Structures*, **19**(6): 485-498.

Hidayat BA, Hu H-T, Hsiao F-P, Han AL, Sosa L, Chan L-Y, Haryanto Y (2021). "Seismic behavior and failure modes of non-ductile three-story reinforced concrete structure: A numerical investigation". *Computers and Concrete*, **27**(5): 457-472.

Hidayat BA, Hu H-T, Hsiao F-P, Shen W-C, Weng P-W, Han AL, Chan L-Y, Haryanto Y (2022). "Modeling of non-ductile RC structure under near-fault ground motions: A nonlinear finite element analysis". *Advances in Structural Engineering*, **25**(9): 1878-1892.

Li B, Siu-Shum Lam E, Wu B and Wang YY (2015). "Effect of high axial load on seismic behavior of reinforced concrete beam-column joints with and without strengthening". *ACI Structural Journal*, **112**(6): 713-724.

Liao WC, Perceka W and Wang M (2017). "Experimental study of cyclic behavior of high-strength reinforced concrete columns with different transverse reinforcement detailing configurations". Engineering Structures, **153**: 290-301.

Park R and Paulay T (1973). "Behaviour of reinforced concrete external beam-column joints under cyclic loading". *5th World Conference on Earthquake Engineering*, 25-29 June, Rome, Italia, 772pp.

Panapa Pita (2018), "Studies on Behavior of Non-ductile Reinforced Concrete Columns and Beam-Column Joints Subjected to Cyclic Loading", Master Thesis, National Cheng Kung University, Taiwan.

Rajput A and Sharma K (2017). "Seismic behavior of under confined square reinforced concrete columns". Structures, **13**: 26-35.

Shafaei J, Hisseini A and Marefat MS (2014). "Seismic retrofit of external RC beam-column joints by joint enlargement prestressed steel angles". *Engineering Structures*, **81**: 265-288.

Shen W-C, Hsiao F-P, Weng P-W, Li Y-A, Chou C-C and Chung L-L (2018). "Seismic tests of a mixed-use residential and commercial building using a novel shaking table". *11th US National Conference on Earthquake Engineering*, 25-29 June, Los Angelos, USA, 4852pp.

Tonidis M, Sharma A, Birtel V (2024). "Experimental and numerical investigations on the influence of transverse beams and slab on the seismic behavior of non-seismically designed exterior beam-column joints". *Earthquake Engineering and Structural Dynamics*, **53**(14): 4451-4476.

Xue Q (2000). "Need of performance-based earthquake engineering in Taiwan: a lesson from the Chi-chi earthquake". *Earthquake Engineering & Structural Dynamics*, **29**: 1609-1627.

Zepeda D and Hagen G (2016). "Lessons learned from the 2016 Taiwan Mei-nong earthquake". *2016 Structural Engineers Association of Southern California Convention*, 12-15 October, Hawaii, USA, 409pp.